Intramolecularly Catalyzed Dynamic Polyester Networks using Neighboring Carboxylic and Sulfonic Acid Groups

Huiyi Zhang[a], Soumabrata Majumdar[a], Rolf A.T.M. van Benthem[a,b], Rint P. Sijbesma[a]* and Johan P.A. Heuts[a]*

[a] Department of Chemical Engineering & Chemistry and Institute for Complex Molecular Systems, Eindhoven University of Technology, PO Box 513, 5600 MB Eindhoven, The Netherlands

[b] DSM Materials Science Center, Urmonderbaan 22, 6167 RD Geleen, The Netherlands

Corresponding authors:

j.p.a.heuts@tue.nl, r.p.sijbesma@tue.nl

Materials

Reagents and solvents were used as received without purification unless otherwise stated.

Tri-arm polycaprolactone star polymer (soft triol, OH value=87.05 mg/KOH/g and acid value=0.05 mg/KOH/g) was kindly provided by Perstorp. Hard polyester triol (OH value=41.70 mg/KOH/g and acid value=2.00 mg/KOH/g) was kindly provided by DSM Coating Resins. Amberlyte IR120 Plus Hydrogen ion exchange resin, pyromellitic dianhydride (PMDA, linker A, 97%), terephthaloyl chloride (linker C, 99%) and 1-hexanol (anhydrous, 99%) were purchased from Sigma Aldrich. Monosodium 2-sulfoterephthalate (98%) and 2-sulfobenzoic anhydride (97%) were purchased from TCI. Toluene and methanol were purchased from Biosolve and kept on 3 Å molecular sieves to maintain dryness.

Syntheses

Synthesis and characterization of 2,5-bis(methoxy-carbonyl) benzene sulfonic acid (linker B, Figure 1)

4 g (14.9 mmol) of monosodium 2-sulfoterephthalate was dissolved in demineralized water and led through a column filled with Amberlyte IR-120 Plus Hydrogen ion exchange resin at room temperature. Water was partly removed under reduced pressure and 2-sulphoterephthalic acid was obtained by freeze drying as a white powder. Then the 2-sulfoterephthalic acid was introduced under argon flow to a 50 mL round bottom flask equipped with a stir bar. To the flask, 20 mL of methanol was charged and the resulting solution was left refluxing for 16 hours. Methanol was then removed *in vacuo* to afford the product as a yellow solid in 95 % yield.

^{1}H NMR (400MHz, DMSO-d_6): δ(ppm) = 3.74 (s, 3H, C*H*3-O), 3.89 (s, 3H, C*H*3-O), 7.42-7.45 (d, 1H, Ar-H), 7.90-7.96 (d, 1H, Ar-H), 8.29-8.32 (s, 1H, Ar-H)

Synthesis and characterization of 2-(hexyloxy-carbonyl) benzene sulfonic acid

1 g (5.4 mmol) of 2-sulfobenzoic anhydride and 5 mL of 1-hexanol were introduced under argon flow to a 25 mL round bottom flask equipped with a stir bar. The mixture was stirred at room temperature for 1 hour. Excess of hexanol was then removed under reduced pressure to afford the product as a yellow solid in 95 % yield.

^{1}H NMR (400MHz, $CDCl_3$): δ(ppm) = 0.87-0.95 (t, 3H, C*H*3CH2), 1.14-1.55 (m, 6H, CH3C*H*2C*H*2C*H*2), 1.76-1.9 (quint, 2H, Ar-H), 7.60-7.86 (m, 2H, Ar-H), 8.01 -8.10 (dd, 1H, Ar-H), 8.19-8.24 (dd, H, Ar-H)

Synthesis of PCL/COOH network

10 g (5.18 mmol) of the tri-arm polycaprolactone star polymer and 30 mL of toluene were charged to a 100 mL round bottom flask equipped with a stir bar under argon flow and stirred at 80 °C until a homogeneous solution was formed. Then 1.41 g (6.47 mmol) of PMDA was added and the resulting mixture was left reacting at 100 °C for 3 hours. Toluene was then removed *in vacuo* at 100 °C overnight to yield the product as a colorless to slightly yellow solid.

Synthesis of PNHTI/COOH network

10 g (2.48 mmol) of the tri-functional copolyester PNHTI precursor and 30 mL of toluene were charged to a 100 mL round bottom flask equipped with a stir bar under argon flow and left stirring at 100 °C until a homogeneous solution was formed. Then 0.68 g (3.1 mmol) of PMDA was added and the resulting mixture was left reacting at 100 °C overnight. Toluene was then removed *in vacuo* at 100 °C overnight to yield the product as a colorless solid.

Synthesis of PCL/SO_3H network

10 g (5.18 mmol) of the tri-arm polycaprolactone star polymer, 1.77 g (6.47 mmol) of linker B and 30 mL of toluene were charged to a 100 mL round bottom flask, and toluene was removed under reduced pressure to dry the reaction mixture. This procedure was repeated, followed by the addition of 30 mL toluene as the reaction solvent. The reaction proceeded under argon flow at 100 °C overnight. Toluene was then removed *in vacuo* at 100 °C overnight to yield a colorless to slightly yellow solid as the product.

Synthesis of PNHTI reference network

10 g (2.48 mmol) of the tri-functional copolyester PNHTI precursor was dissolved in 30 mL of toluene in a 100 mL round bottom flask. Toluene was then removed under reduced pressure to dry the polymer. This procedure was repeated, followed by the addition of 0.632 g (3.1 mmol) of linker C and 30 mL of toluene into the round bottle flask. The reaction proceeded after charging a stir bar under heavy argon flow at 100 °C overnight. Toluene was then removed *in vacuo* at 100 °C overnight to yield a colorless to slightly yellow solid as the product.

Characterization

Dynamic mechanical analysis (DMA)

Compression molded samples (ca. 10.0 (length) × 10.0 (width) × 0.8 (thickness) mm) were measured on a DMA Q850 (TA Instruments) with a film tension setup. A temperature ramp from -60 to 200 °C was performed with a heating rate of 3 °C·min^{-1} at a frequency of 1 Hz. A preload force of 0.01 N, an amplitude of 10 µm and a force track of 110% were used. The storage and loss moduli were recorded as a function of temperature. The glass transition temperature was determined from the peak maximum in the loss modulus.

Gel fraction determination

Approximately 0.15 g of the dry network was weighed and swollen in 20 mL of $CHCl_3$ and kept for 3 days at room temperature, the sample was subsequently filtered and dried in a vacuum oven at 100 °C for 24 hours. The gel fraction was calculated with the equation (**Eq S1)**, where $m_{initial}$ is the mass of the sample before extraction and m_{dry} is the mass after extraction and drying:

$$\text{gel fraction (\%)} = \frac{m_{dry}}{m_{initial}} \times 100\% \quad \text{(S1)}$$

Stress relaxation and frequency sweep experiments

All rheological measurements were carried out on a strain-controlled AR-G2 rheometer with an ETC oven setup (TA Instruments) and parallel-plate geometry. A typical sample for rheology measurements was approximately 8 mm in diameter and 0.8 mm thick, prepared by compression molding the dry product at 180 °C and a pressure of 100 bar for 15 min. For all measurements, a constant range of normal force of 10 ± 2 N was applied by automatically adjusting the gap to ensure proper contact between the sample and plates. A thermal treatment of 20 min at 200 °C was applied to the PNHTI-based samples and 180 °C for the PCL-based samples prior to conditioning at the measurement temperature to eliminate potential differences in the degrees of curing and to eliminate any surface roughness of the highly cross-linked sample. Stress relaxation data for all samples were collected at a step strain of 1% (within linear viscoelastic regime). The relaxation modulus $G(t)$ was monitored for various amount of time depending on the temperature. Frequency sweeps for the samples were carried out at 1% of strain in the frequency range from 100 rad/s to 0.001 rad/s.

Thermogravimetric analysis (TGA)

Thermal stability studies were performed on a TA Instruments TGA Q500 instrument under a N_2 rich atmosphere. Samples were heated at 10 °C $\cdot min^{-1}$ from 20 to 600 °C. Temperature calibration was performed using the Curie points of high purity aluminum, nickel and perkalloy standards.

Proton nuclear magnetic resonance spectroscopy (^{1}H-NMR)

^{1}H-NMR spectroscopy measurements were performed on a 400 MHz Bruker Avance III spectrometer at 25 °C, with a spectral width of 6402 Hz, a delay time of 5 s and a number of scans of 64. Tetramethylsilane (TMS) was used as the standard (δ= 0 ppm).

Differential scanning calorimetry (DSC)

DSC measurements were performed on a TA Instruments Q2000 differential scanning calorimeter equipped with an RCS90 cooling accessory using aluminium hermetic pans. For each measurement, 5-10 mg of sample was used. The sample was scanned twice from -80 °C to 200 °C at a heating rate of 20 °C/min, followed by a cooling cycle in the sample temperature range at a rate of 20 °C/min. T_g was determined as the midpoint of the step in the heat flow curve, analysed using TA Universal Analysis software.

Variable Temperature Infrared Spectroscopy (VT-IR)

VT-IR spectra were recorded on a JASCO Tensor 27 with Pike ATR temperature unit. For each measurement, the sample was scanned from 40 °C to 200 °C at a heating rate of 5 °C/min under N_2 flow. Background spectra at varying temperature were recorded under the same conditions and subtracted from the recorded raw spectra using OriginLab to obtain the final spectra.

Results

NMR spectra

The ^{1}H NMR spectra of 2,5-bis(methoxy-carbonyl) benzene sulfonic acid (linker B) and 2-((hexyloxy)carbonyl) benzene sulfonic acid (the model compound used in the VT-FTIR measurements) are shown in Figure S1.

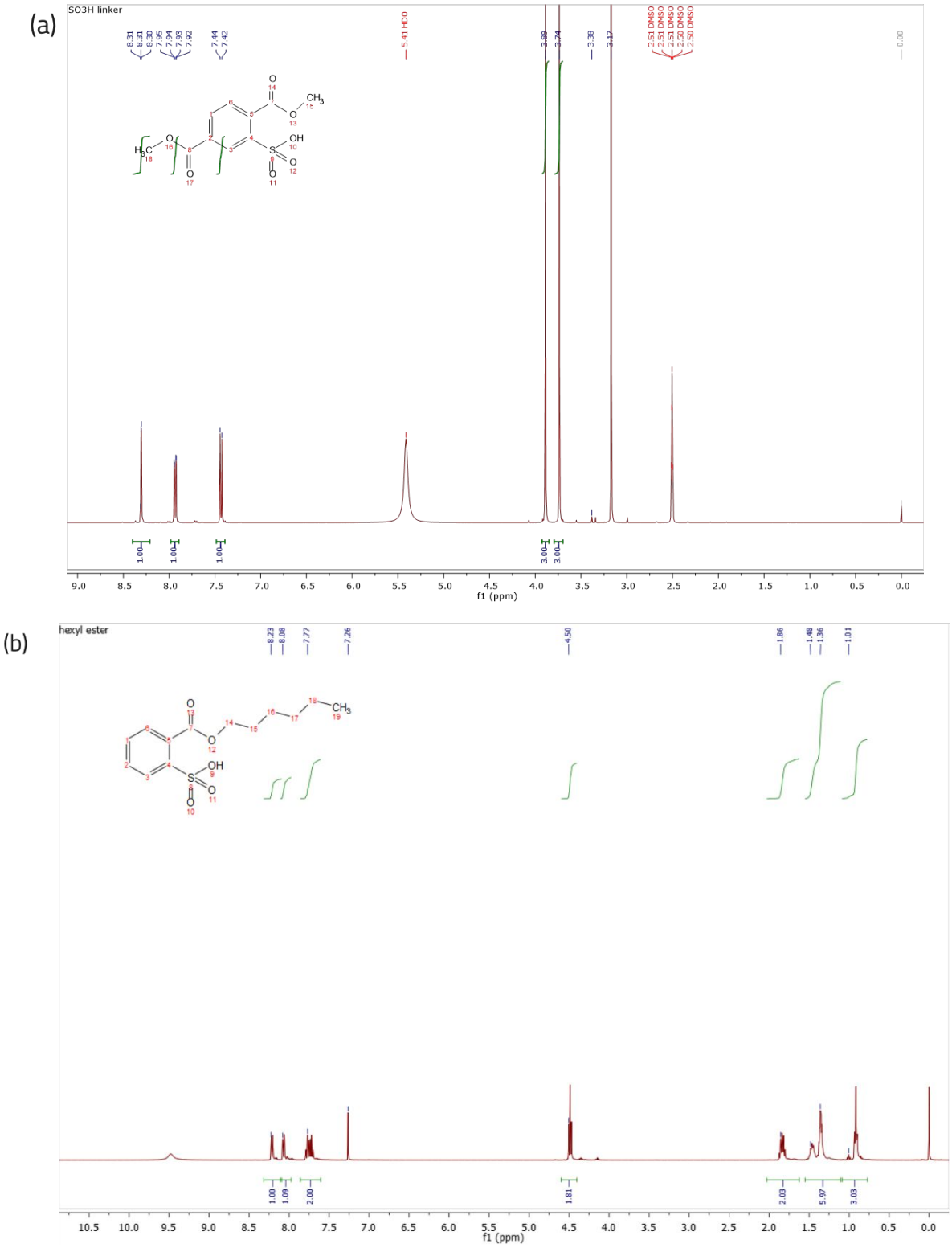

Figure S1 ^{1}H-NMR spectra of (a) 2,5-bis(methoxy-carbonyl) benzene sulfonic acid (linker B) in DMSO-d_6 and (b) 2-((hexyloxy)carbonyl)benzene sulfonic acid in $CDCl_3$.

Thermal properties and gel contents

Thermal properties and gel contents of the synthesized dynamic networks and their precursors are listed in Table S1. The parameter *r* is the ratio of the number of OH-end groups to linker molecules.

Table S1 Thermal properties and gel content of polyester networks.

Composition	$r = n_{OH}/n_{linker}$	T_{d5}(°C)	T_g (°C) DSC	T_g (°C) DMA	Gel content (%)
PCL/COOH	2.4	253	0	N.A.	97
PCL/SO_3H	2.4	234	0	N.A.	90
PCL-reference with 0.5 mol% $Zn(acac)_2$	2.4	373	9	N.A.	95
PCL-reference with 2.0 mol% $Zn(acac)_2$	2.4	205	9	N.A.	94
PCL precursor	—	325	-63	N.A.	0
PNHTI/COOH	2.4	321	50	54	90
	2.2	310	54	64	91
	2.0	322	59	76	95
	1.9	325	58	63	92
PNHTI/SO_3H	2.4	278	47	53	90
	2.2	272	48	61	90
PNHTI precursor	—	357	39	N.A.	0

Stress relaxation experiments

All samples were subjected to a thermal pre-treatment before stress relaxation experiments prior to conditioning at the measurement temperature: 20 min at 200°C for the PHNTI-based samples and 20 min at 180°C for the PCL-based samples. A representative measurement of the relaxation modulus is shown in Figure S2a and it can be seen that a stable signal is obtained within 1 s after the start of the measurement. We therefore choose the moduli at t = 1 s as the initial moduli G_0, which were used to construct the normalized stress relaxation curves. The normalized curve of the relaxation modulus of Figure S2a is shown in Figure S2b and it is clear that the stresses are fully relaxed in the material.

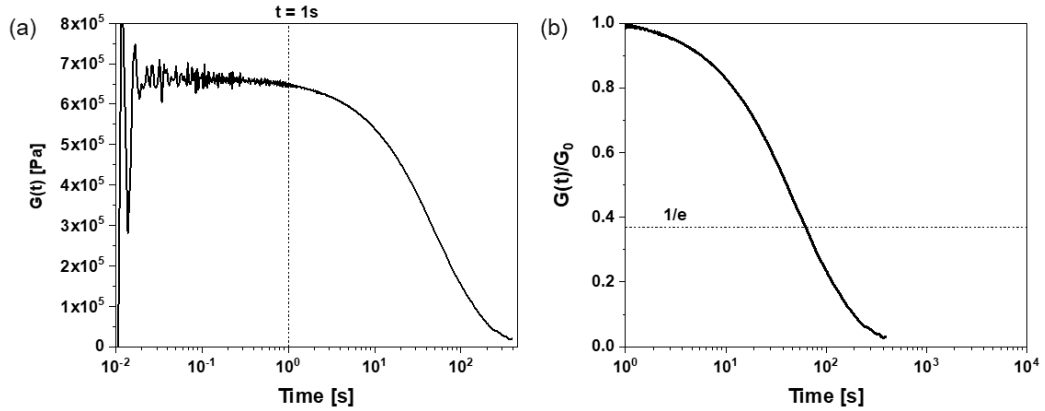

Figure S2 (a) A representative stress relaxation curve, where a step strain is applied at t = 0.01 s and the $G(t)$ levels out within the first second; and (b) the corresponding stress relaxation curve after normalizing $G(t)$ against G(t = 1s). Sample: PCL-based network with linker B and $r = n_{OH} / n_{linker}$ = 2.4.

A comparison of the stress relaxation curves of the networks produced from the two precursors and different linkers is shown in Figures 2a and 2b of the manuscript. Here we show the same data in "log-linear" plots, together with model fits according to a simple Maxwell model (Eq. S2) and a stretch exponential (Eq. S3):

Maxwell: $$\frac{G(t)}{G_0} = e^{-t/\tau^*} \quad \text{(S2)}$$

Stretched exponential: $$\frac{G(t)}{G_0} = e^{-\left(t/\tau^*\right)^{\beta}} \quad \text{(S3)}$$

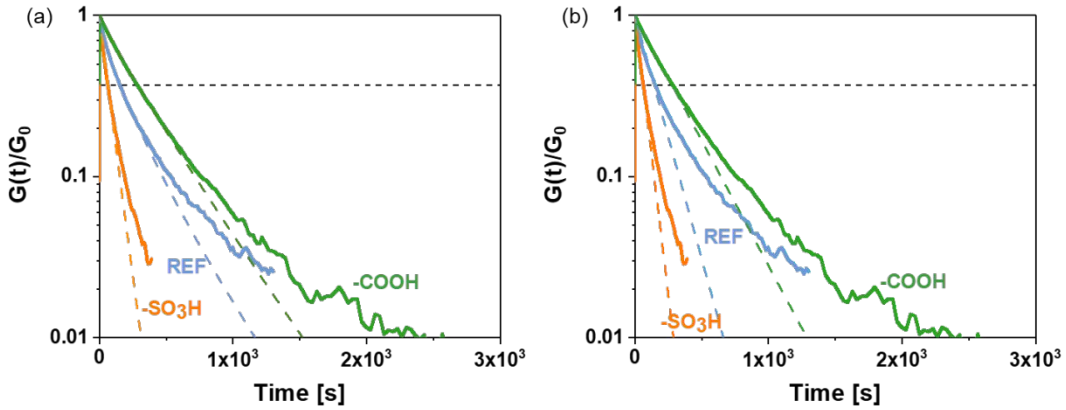

Figure S3 Oscillatory rheology stress relaxation experiments (1% step strain) on PCL-based networks with different linkers ($r = n_{OH}/n_{linker}$ = 2.4) at 180 °C (a) including fits using Eq S2 (dotted lines), and (b) including fits using Eq S3 (dotted lines). The intersections of the horizontal dotted lines with the stress relaxation curves indicate the points where $G(t)/G_0$ = 1/e. REF represents the reference network with 2 mol% $Zn(acac)_2$.

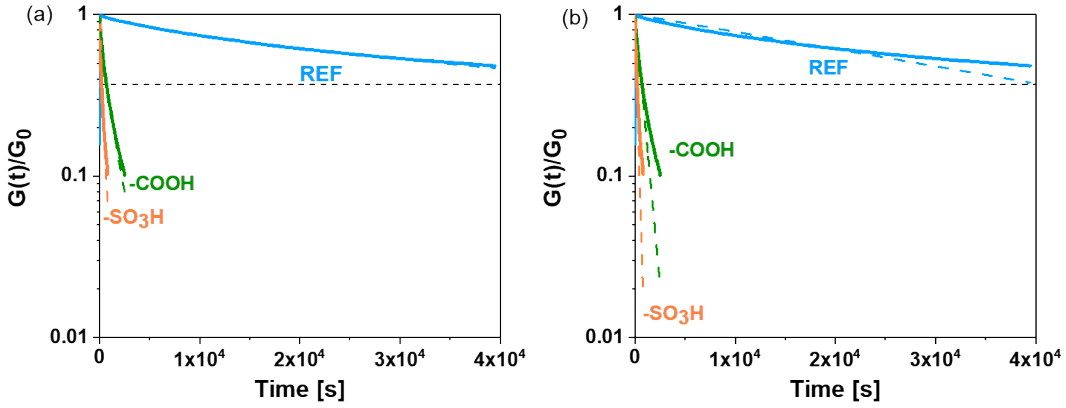

Figure S4 Oscillatory rheology stress relaxation experiments (1% step strain) on PNHTI-based networks with different linkers ($r = n_{OH}/n_{linker}$ = 2.4) at 180 °C (a) including fits using Eq S2 (dotted lines), and (b) including fits using Eq S3 (dotted lines). The intersections of the horizontal dotted lines with the stress relaxation curves indicate the points where $G(t)/G_0$ = 1/e. REF represents the reference network with 2 mol% $Zn(acac)_2$.

The fit parameters of the model fits shown in Figures S3 and S4, together with experimental values of τ* (determined as the time at which $G(t)/G_0$ = 1/e) are listed in Table S2. It is clear from these results that the characteristic relaxation times from both models are very close and close to the experimentally determined values. Also the "stretch exponents" □ are all very high, with those of the PCL-based systems very close to 1. We therefore decided to base the analysis of the temperature dependence of the stress relaxation on the experimental values for τ*.

Table S2 Fit results for stress relaxation experiments at 180°C for networks with $r = n_{OH}/n_{linker}$ = 2.4

Composition network	Experimental τ* (s)	Maxwell (Eq S2) τ* (s)	Stretched exponential (Eq S3) τ* (s)	β
PCL/SO_3H	63	63	64	0.96
PCL/COOH	$2.8 \cdot 10^2$	$2.8 \cdot 10^2$	$2.9 \cdot 10^2$	0.92
PCL reference with 2mol% $Zn(acac)_2$	$1.5 \cdot 10^2$	$1.4 \cdot 10^2$	$1.6 \cdot 10^2$	0.77
PNHTI/SO_3H	$2.1 \cdot 10^2$	$2.0 \cdot 10^2$	$2.2 \cdot 10^2$	0.76
PNHTI/COOH	$7.0 \cdot 10^2$	$6.5 \cdot 10^2$	$7.2 \cdot 10^2$	0.75
PNHTI reference with 2mol% $Zn(acac)_2$	not available	$42 \cdot 10^3$	$58 \cdot 10^3$	0.70

The temperature dependences of the stress relaxation curves for a range of PCL-based and PNHTI-based dynamic networks with different linkers and different cross-link densities are shown in Figures S5 - S7. The Arrhenius plots in Figure 2 of the manuscript are based on these results.

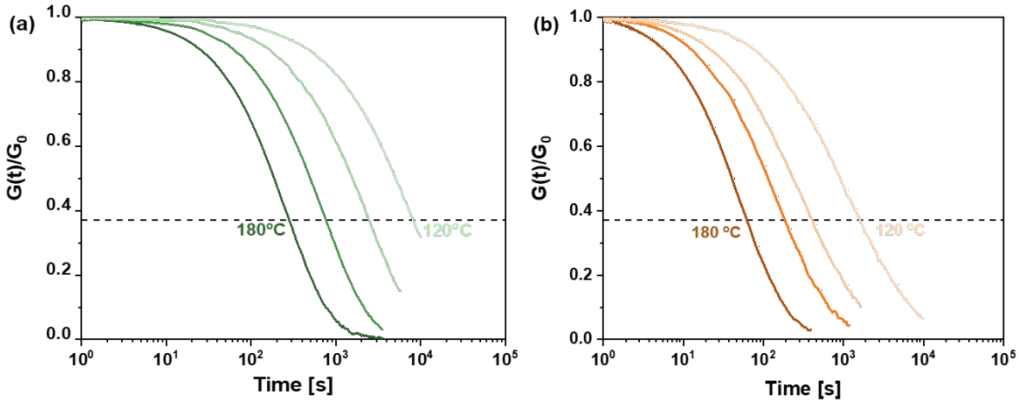

Figure S5 Oscillatory rheology stress relaxation experiments (1% step strain) of (a) PCL/COOH and (b) PCL/SO_3H networks with $r = n_{OH} / n_{linker}$ = 2.4 at varying temperatures. The intersections of the horizontal dotted lines with the stress relaxation curves indicate the points where $G(t)/G_0$ = 1/e and t = τ*.

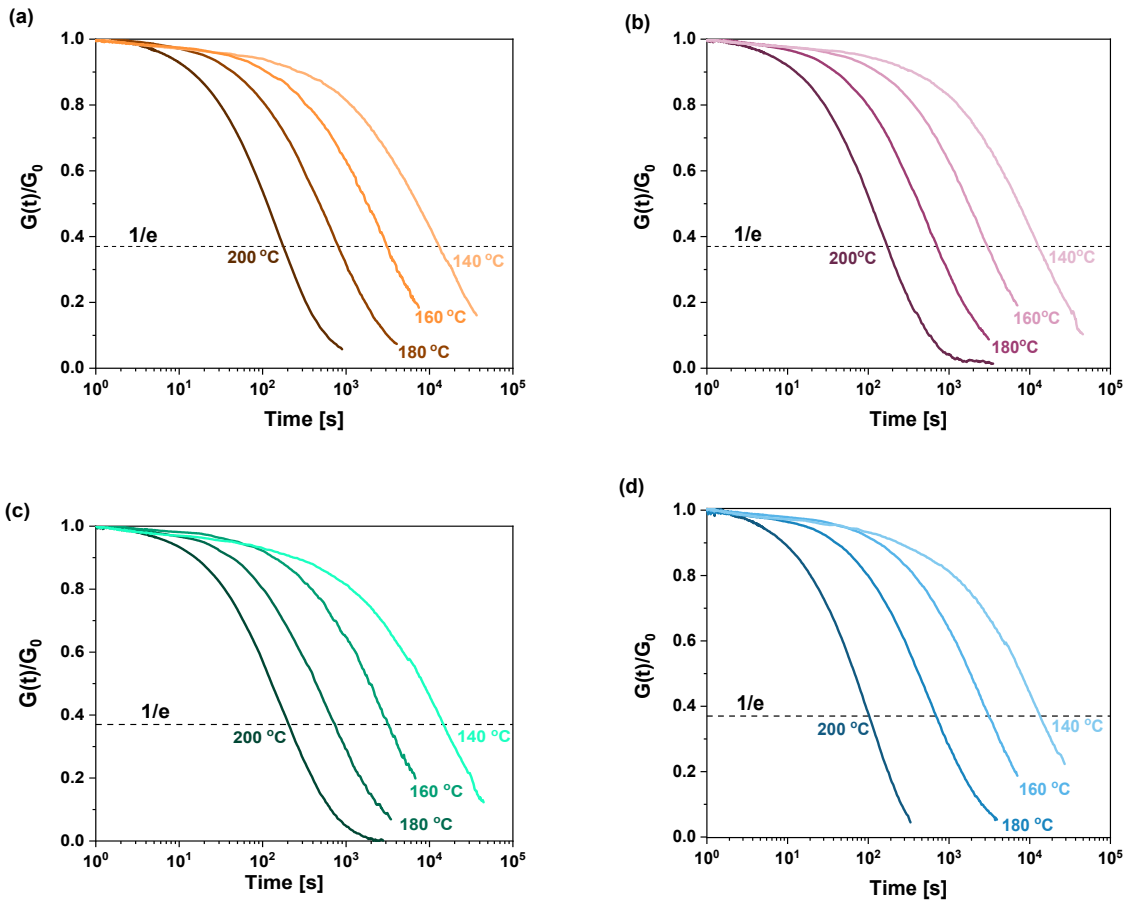

Figure S6 Oscillatory rheology stress relaxation experiments (1% step strain) of PNHTI/COOH networks with r = n_{OH} / n_{linker} = (a) 2.2 (b) 2, (c) 1.9, (d) 2.4 at varying temperatures. The intersections of the horizontal dotted lines with the stress relaxation curves indicate the points where $G(t)/G_0$ = 1/e and t = τ*.

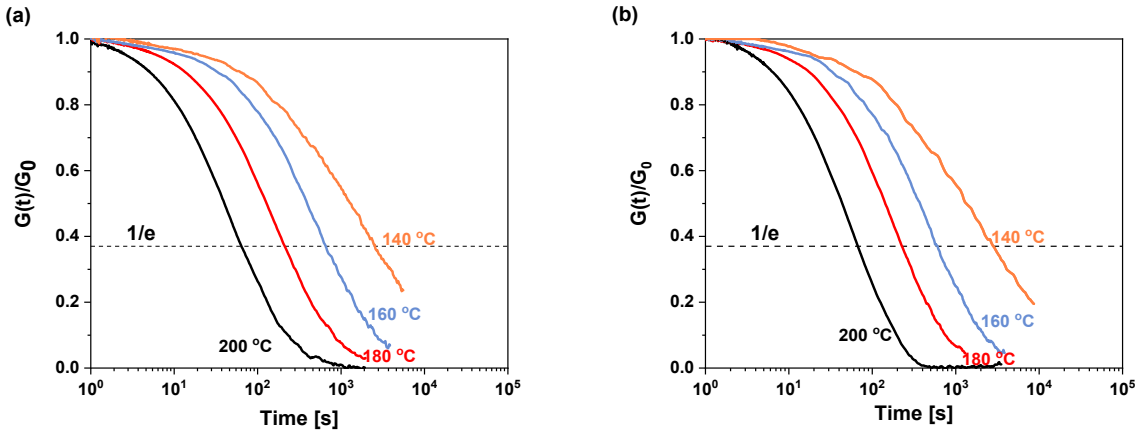

Figure S7 Oscillatory rheology stress relaxation experiments (1% step strain) of PNHTI/SO_3H networks with r with r = n_{OH} / n_{linker} = (a) 2.4, (b) 2.2 at varying temperatures. The intersections of the horizontal dotted lines with the stress relaxation curves indicate the points where $G(t)/G_0$ = 1/e and t = τ*.

Frequency sweep measurements on the PCL/COOH network (r = 2.4)

Frequency sweeps in oscillatory shear experiments at a strain of 1% were carried out in the temperature range between 120 and 200°C to probe the time-temperature dependent dynamic mechanical properties. The results of these experiments are shown in Figure S8. This sample displays an almost frequency-independent rubber plateau modulus G' ≈ 2 MPa at T = 120°C. At $T \geq$ 140°C a decrease in G' w.r.t. the plateau value is observed for increasingly high frequency with increasing temperature as is best seen from the normalized data shown in Figure S8c; this is indeed what is expected for a dynamic covalent network. Obviously this is also seen in the raw data in Figure S8b, but the small scatter in the plateau modulus obscures this effect a little. This scatter also precludes us from drawing the conclusion that at higher temperatures, the plateau modulus decreases in dissociative dynamic covalent networks (because of a decrease in cross-link density). Associative networks would not show this decrease. Although our data seem to hint at a lower cross-link density at higher temperatures, there is too much scatter to conclude this with certainty.

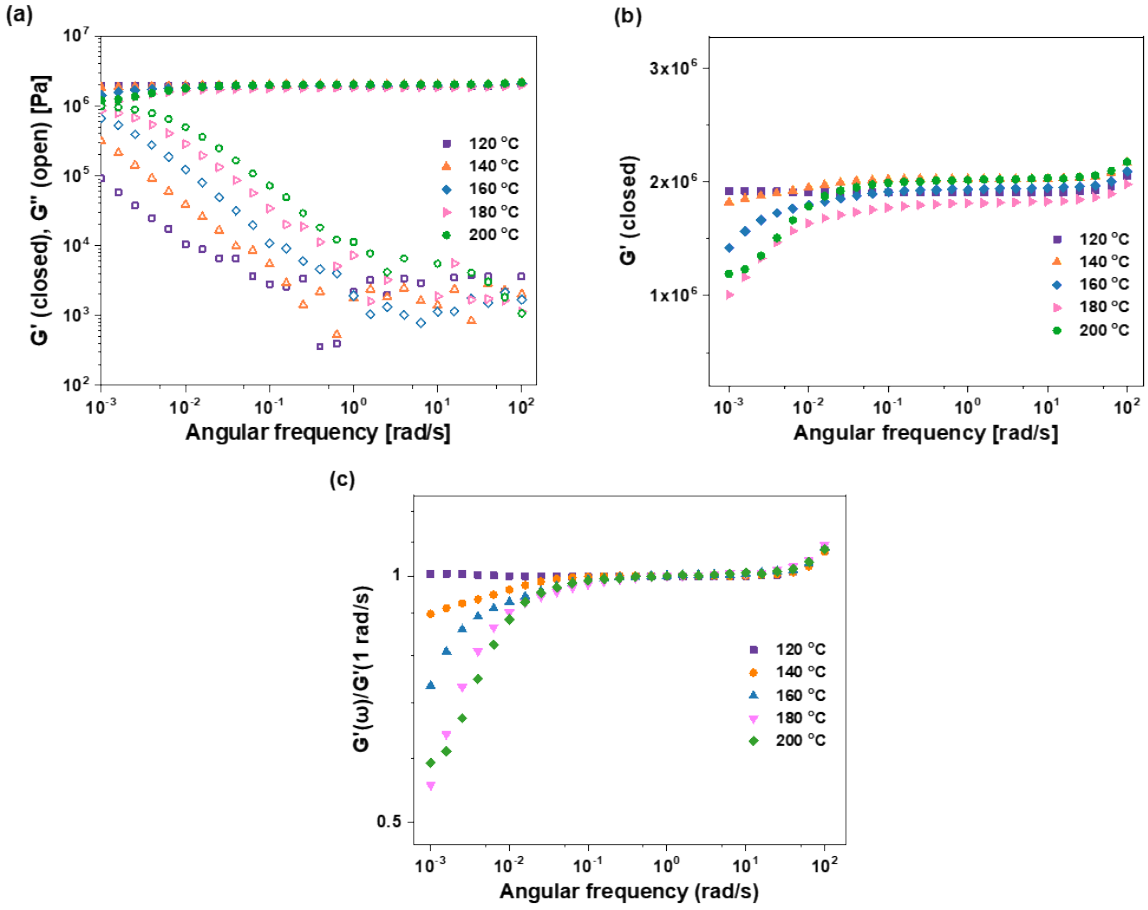

Figure S8 (a) Frequency dependence of the moduli of PCL/COOH network with $r = n_{OH} / n_{linker}$ = 2.4 at varying temperatures, (b) amplification of the storage moduli data of figure a and (c) the normalized storage moduli against $G'(\omega = 1$ rad/s) at varying temperatures.

Potential side reactions leading to reduced dynamics

The dynamic behavior in the reported polyester network arises from the formation of anhydrides from esters with neighboring acid groups under expulsion of an alcohol. This mechanism had already been shown by Du Prez' group for the PMDA based linker system (see Figure 1b in the manuscript) and is demonstrated for neighboring sulfonic acid groups in the current work. In the system with neighboring COOH groups, ideally the system would only contain 1,4- and 1,3-diesters (see Table S3, where R is a connecting chain). These sub-units contain two esters with neigboring acid groups, so both esters can undergo transesterification reactions with anhydride intermediates (intramolecular catalysis by the COOH groups). Further esterification of one of the acid groups in a 1,4- or 1,3-diester leads to a 1,2,4-triester (see Table S3), leading to a subunit in which only one ester group has a neighboring acid group to promote transesterification via an anhydride intermediate. The other two ester groups are unreactive in the absence of an external transesterification catalyst and hence this particular subunit only has 1 of 2 dynamic sites left. In a tetraester sub-unit (Table S3) reversibility is fully lost. Finally, hydrolysis of ester groups or anhydrides (*e.g.* from water that is formed during an esterification reaction), may lead to a structure such as the 1,2-diester, in which intramolecular catalysis of the ester exchange does also not occur.

Since formation of sulfonic esters is much less favorable,[1] deactivating side reactions will not take place in the networks with neighboring sulfonic acid groups.

Table S3 The structure and reversibility of possible linkages in COOH networks.

Structure		Dynamic nature
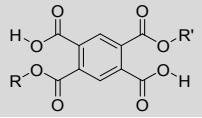	1,4-diester	Reversible
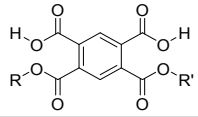	1,3-diester	Reversible
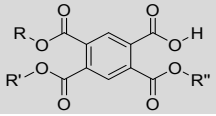	1,2,4-triester	Reduced reversibility
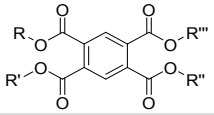	tetraester	Irreversible
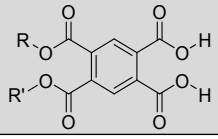	1,2-diester	Reduced reversibility

Variable temperature infrared spectroscopy

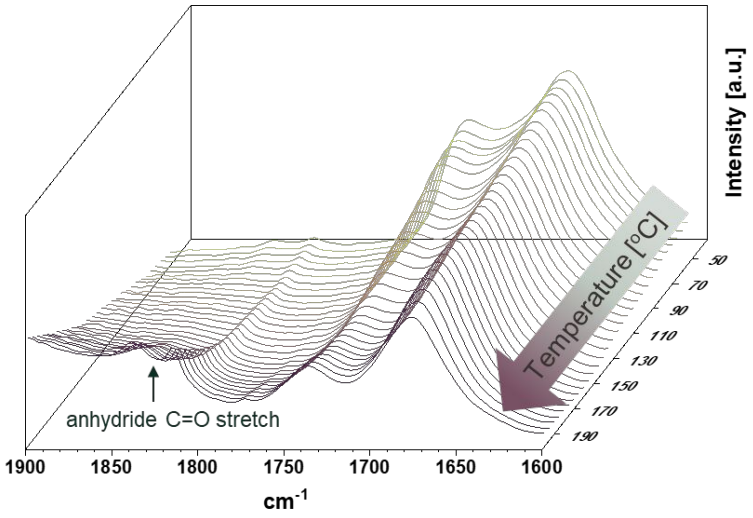

Figure S9 Variable temperature infrared spectra of 2-sulfo hexyl phthalate, collected from 40°C to 200°C under N_2 at a heating rate of 5 °C/min.

Comparison with other dynamic network systems

In Table S4 the relaxation times at 140°C and activation energies of our current systems are compared with a (random) selection of other systems, including a range of other dynamic systems based on trans reactions and catalyst-free systems.

Table S4 A comparison of a selection of dynamic polymer network systems at 140°C

System	External Catalyst	τ (140°C)[a]	E_a[b] (kJ/mol)	Ref.
Boroxine network boroxine exchange	none	0.5 s[d]	80	**2**
Polylactide transesterification	$Sn(Oct)_2$ 5 mol% wrt OH	22 s	150	**3**
PMMA vitrimer dioxaborolane metathesis	none	69 s	77	**4**
Poly(4-methylcaprolactone) transesterification	Benzene sulfonic acid 3 mol% wrt ester	79 s[d]	56	**5**
Polyhydroxyurethane w/ disulfide exchange	none	90 s	78	**6**
Poly(alkylurea-urethane) urethane exchange	none	94 s[d]	59	**7**
Vinylogous urethane transamination	none	360 s[d]	60	**8**
PCL/SO_3H transesterification	none	403 s	78	**this work**
PCL/ref transesterification	$Zn(acac)_2$ 2 mol% wrt ester	$1.7 \cdot 10^3$ s	93	**this work**
Poly(thioethers) transalkylation	none	$1.7 \cdot 10^3$ s[d]	113	**9**
DEPD polyester/COOH [c] transesterification	none	$2 \cdot 10^3$ s	120	**10**
PCL/COOH transesterification	none	$2.5 \cdot 10^3$ s	84	**this work**
PHNTI/SO_3H transesterification	none	$2.5 \cdot 10^3$ s	98	**this work**
Dynamic thioester network trans thioesterification	DABCO 3 mol% wrt thioester	$2.7 \cdot 10^3$ s[e]	N.A.	**11**
PHNTI/COOH transesterification	none	$1.4 \cdot 10^4$ s	116	**this work**
DGEBA epoxy-anhydride transesterification	$Zn(acac)_2$ 5 mol% wrt ester	$1.8 \cdot 10^4$ s	80	**12**
Hyperbranched epoxy transesterification	none	$3.0 \cdot 10^4$ s[d]	63	**13**
Polyhydroxypolyurethane vitrimer transcarbamoylation	none	$4.5 \cdot 10^4$ s[d]	111	**14**
Poly(butylene terephthalate) transesterification	$Zn(acac)_2$ 2 mol% wrt ester	$2 \cdot 10^6$ s[d,f]	155	**15**

[a] Approximate characteristic relaxation times, τ, ($G(t)/G_0$ = 1/e) at 140°C; [b] approximate activation energies for τ; [c] intramolecular catalysis via same mechanism as this work; [d] τ estimated from reported Arrhenius parameters; [e] value at room temperature; [f] this value is only a theoretical value, because at 140°C these vitrimers are below their melting point ($\tau \approx 10^2$ s at 270°C).

References

1. Guthrie, J. P., Hydrolysis of esters of oxy acids: pKa values for strong acids; Brønsted relationship for attack of water at methyl; free energies of hydrolysis of esters of oxy acids; and a linear relationship between free energy of hydrolysis and pKa holding over a range of 20 pK units. *Canadian Journal of Chemistry* **1978**, *56* (17), 2342-2354.

2. Ogden, W. A.; Guan, Z., Recyclable, strong and highly malleable thermosets based on boroxine networks. *Journal of the American Chemical Society* **2018,** *140* (20), 6217-6220.

3. Brutman, J. P.; Delgado, P. A.; Hillmyer, M. A., Polylactide Vitrimers. *ACS Macro Letters* **2014,** *3* (7), 607-610.

4. Röttger, M.; Domenech, T.; van der Weegen, R.; Breuillac, A.; Nicolaÿ, R.; Leibler, L., High-performance vitrimers from commodity thermoplastics through dioxaborolane metathesis. *Science* **2017,** *356* (6333), 62-65.

5. Self, J. L.; Dolinski, N. D.; Zayas, M. S.; Read de Alaniz, J.; Bates, C. M., Brønsted-Acid-Catalyzed Exchange in Polyester Dynamic Covalent Networks. *ACS Macro Letters* **2018,** *7*, 817-821.

6. Fortman, D. J.; Snyder, R. L.; Sheppard, D. T.; Dichtel, W. R., Rapidly Reprocessable Cross-Linked Polyhydroxyurethanes Based on Disulfide Exchange. *ACS Macro Letters* **2018,** *7* (10), 1226-1231.

7. Zhang, L.; Rowan, S. J., Effect of Sterics and Degree of Cross-Linking on the Mechanical Properties of Dynamic Poly(alkylurea–urethane) Networks. *Macromolecules* **2017,** *50* (13), 5051-5060.

8. Denissen, W.; Rivero, G.; Nicolaÿ, R.; Leibler, L.; Winne, J. M.; Du Prez, F. E., Vinylogous Urethane Vitrimers. *Advanced Functional Materials* **2015,** *25* (16), 2451-2457.

9. Hendriks, B.; Waelkens, J.; Winne, J. M.; Du Prez, F. E., Poly(thioether) Vitrimers via Transalkylation of Trialkylsulfonium Salts. *ACS Macro Letters* **2017,** *6* (9), 930-934.

10. Delahaye, M.; Winne, J. M.; Du Prez, F. E., Internal catalysis in covalent adaptable networks: phthalate monoester transesterification as a versatile dynamic crosslinking chemistry. *Journal of the American Chemical Society* **2019**, *141* (38), 15277-15287.

11. Worrell, B. T.; Mavila, S.; Wang, C.; Kontour, T. M.; Lim, C.-H.; McBride, M. K.; Musgrave, C. B.; Shoemaker, R.; Bowman, C. N., A user's guide to the thiol-thioester exchange in organic media: scope, limitations, and applications in material science. *Polymer Chemistry* **2018,** *9* (36), 4523-4534.

12. Montarnal, D.; Capelot, M.; Tournilhac, F.; Leibler, L., Silica-Like Malleable Materials from Permanent Organic Networks. *Science* **2011,** *334* (6058), 965-968.

13. Han, J.; Liu, T.; Hao, C.; Zhang, S.; Guo, B.; Zhang, J., A Catalyst-Free Epoxy Vitrimer System Based on Multifunctional Hyperbranched Polymer. *Macromolecules* **2018,** *51* (17), 6789-6799.

14. Fortman, D. J.; Brutman, J. P.; Cramer, C. J.; Hillmyer, M. A.; Dichtel, W. R., Mechanically Activated, Catalyst-Free Polyhydroxyurethane Vitrimers. *Journal of the American Chemical Society* **2015,** *137* (44), 14019-14022.

15. Zhou, Y.; Goossens, J. G. P.; Sijbesma, R. P.; Heuts, J. P. A., Poly(butylene terephthalate)/Glycerol-based Vitrimers via Solid-State Polymerization. *Macromolecules* **2017,** *50* (17), 6742-6751.